Biochemical evidence for conformational variants in the anti-viral and pro-metastatic protein IFITM1

Marta Nekulová, Marta Wyszkowska, Nela Friedlová, Lukáš Uhrík, Filip Zavadil Kokáš, Václav Hrabal, Lenka Hernychová, Bořivoj Vojtěšek, Ted R. Hupp and Michał R. Szymański*

Biochemical evidence for conformational variants in the anti-viral and pro-metastatic protein IFITM1

https://doi.org/10.1515/hsz-2023-0327
Received October 16, 2023; accepted January 30, 2024;
published online February 22, 2024

Abstract: Interferon induced transmembrane proteins (IFITMs) play a dual role in the restriction of RNA viruses and in cancer progression, yet the mechanism of their action remains unknown. Currently, there is no data about the basic biochemical features or biophysical properties of the IFITM1 protein. In this work, we report on description and biochemical characterization of three conformational variants/oligomeric species of recombinant IFITM1 protein derived from an *Escherichia coli* expression system. The protein was extracted from the membrane fraction, affinity purified, and separated by size exclusion chromatography where two distinct oligomeric species were observed in addition to the expected monomer. These species remained stable upon re-chromatography and were designated as "dimer" and "oligomer" according to their estimated molecular weight. The dimer was found to be less stable compared to the oligomer using circular dichroism thermal denaturation and incubation with a reducing agent. A two-site ELISA and HDX mass spectrometry suggested the existence of structural motif within the N-terminal part of IFITM1 which might be significant in oligomer formation. Together, these data show the unusual propensity of recombinant IFITM1 to naturally assemble into very stable oligomeric species whose study might shed light on IFITM1 anti-viral and pro-oncogenic functions in cells.

Keywords: hydrogen deuterium exchange; IFITM proteins; oligomerization; protein conformation; protein structure

1 Introduction

Interferon induced transmembrane proteins (IFITMs) are small homologous proteins that are localized in the endosomal and plasma membranes and expressed in many cell types including barrier epithelial cells and immune cells (Bailey et al. 2014; Smith et al. 2006). The IFITM family includes five homologs in humans that differ in their expression patterns in normal and tumor tissues, intracellular localization and functions (Smith et al. 2006; Weston et al. 2014). The three most studied members of this protein family, IFITM1, IFITM2 and IFITM3, were initially identified almost 40 years ago (Friedman et al. 1984) as products of genes strongly upregulated by interferons, and were subsequently defined as antiviral restriction factors (Brass et al. 2009). They have broad-spectrum antiviral activity and are unique in their ability to block viral entry through lipid bilayer to the cytoplasm (Bailey et al. 2014; Diamond and Farzan 2013; Smith et al. 2014; Zhao et al. 2019). IFITM proteins are also often overexpressed in cancer cells (Friedlová et al. 2022; Liang et al. 2020), play an important role in adaptive immunity (Yánez et al. 2020), and are associated with germ cell specification (Lange et al. 2003; Tanaka et al. 2005).

Based on the structural predictions, IFITM proteins are built of distinct domains, N-terminal domain (NTD), intramembrane domain (IMD), conserved intracellular loop (CIL), transmembrane domain (TMD) and C-terminal domain (CTD) (Zhao et al. 2019) (Figure 1A and B). A proposed model of the protein topology in a membrane environment shows that NTD is exposed intracellularly, IMD is connected with TMD via CIL, while CTD resides on the extracellular surface of the plasma membrane (Figure 1A) (Sun et al. 2020; Weston et al. 2014). The combined homology of IMD and CIL defines the highly conserved CD225 domain, which is shared by the members of the CD225/dispanin family (IPR007593; (Paysan-Lafosse et al. 2023)). In contrast, IFITM N-terminal and C-terminal domains

Marta Nekulová and Marta Wyszkowska contributed equally to this work.

***Corresponding author: Michał R. Szymański**, Structural Biology Laboratory, Intercollegiate Faculty of Biotechnology of University of Gdansk and Medical University of Gdansk, University of Gdansk, Abrahama 58/207A, 80-307 Gdansk, Poland, E-mail: michal.szymanski@ug.edu.pl
Marta Nekulová, Lukáš Uhrík, Filip Zavadil Kokáš, Lenka Hernychová and Bořivoj Vojtěšek, Research Centre for Applied Molecular Oncology, Masaryk Memorial Cancer Institute, 656 53 Brno, Czech Republic. https://orcid.org/0000-0001-6404-2566 (M. Nekulová)
Marta Wyszkowska, Structural Biology Laboratory, Intercollegiate Faculty of Biotechnology of University of Gdansk and Medical University of Gdansk, University of Gdansk, 80-307 Gdansk, Poland
Nela Friedlová and Václav Hrabal, Research Centre for Applied Molecular Oncology, Masaryk Memorial Cancer Institute, 656 53 Brno, Czech Republic; and Department of Experimental Biology, Faculty of Science, Masaryk University, 625 00 Brno, Czech Republic
Ted R. Hupp, Institute of Genetics and Molecular Medicine, University of Edinburgh, EH4 2XR Edinburgh, UK

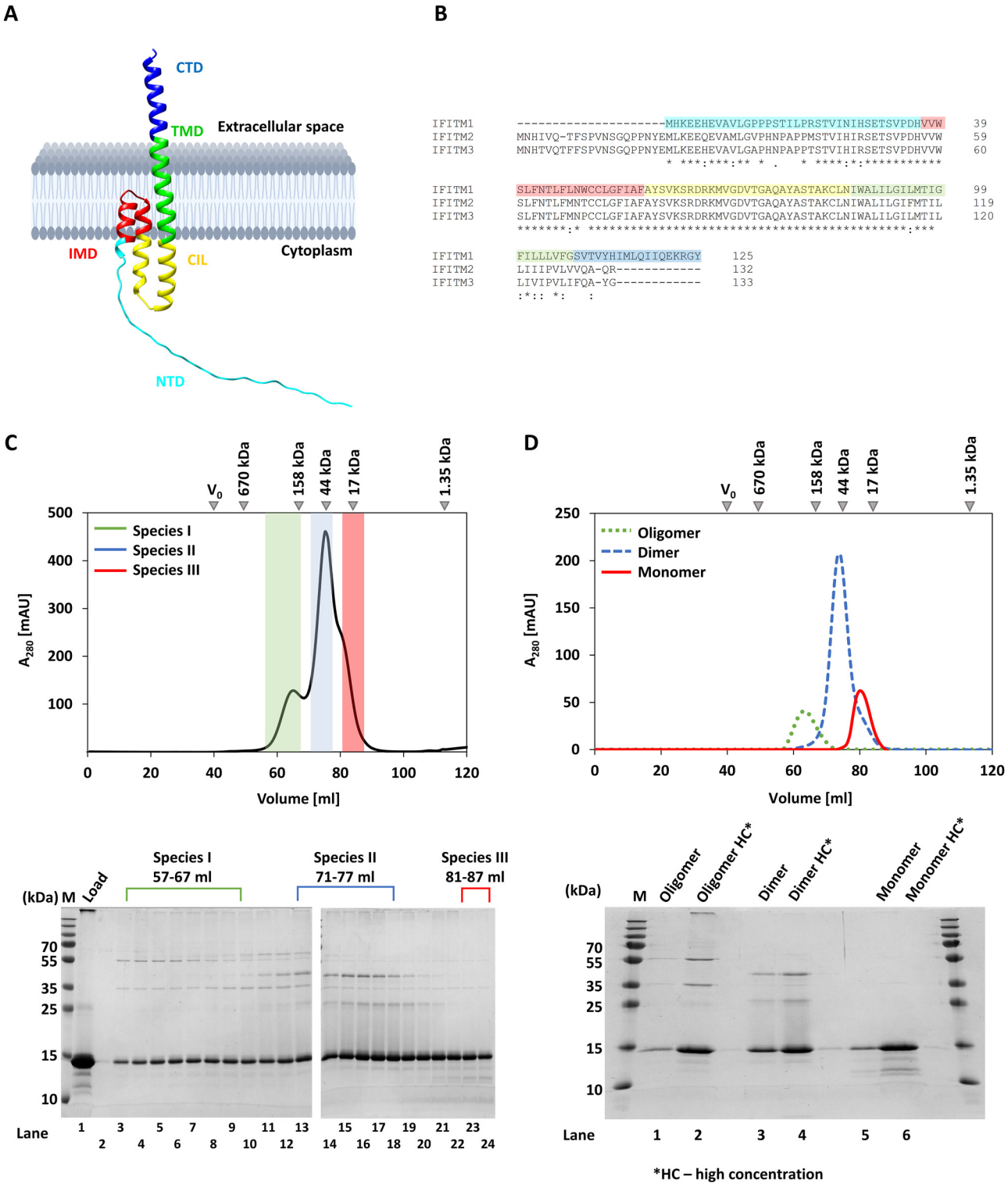

Figure 1: IFITM1 protein forms stable, separate oligomeric species. (A) Model of topology of monomeric IFITM1 protein in a membrane based on the prediction using AlphaFold (accession in UniProt: P13164). Five domains of IFITM1 are distinguished: Cytoplasmic NTD in cyan, IMD in red, CIL in yellow, TMD in green and CTD protruding outside of the cell in dark blue. (B) Sequence alignment of IFITM1, IFITM2 and IFITM3. An asterisk (*) indicates conserved amino acid at that position, a colon (:) indicates conservative substitution and blank space ( ) indicates non-conservative substitution. (C) SEC elution profile of combined oligomeric species. Peaks are marked with colours: Species I (green), species II (blue), species III (red) (top panel). SDS-PAGE analysis of SEC fractions (bottom panel). Oligomeric species and their elution volumes are marked with colours corresponding to peaks on the graph C. (D) Separated oligomeric species of IFITM1 obtained during second round of analytical SEC. Peaks are marked with colours: Oligomer (dotted green line), dimer (dashed blue line), monomer (red line) (top panel). SDS-PAGE gel analysis of separated oligomeric species in low and high concentration (bottom panel).

display heterogeneity in both sequence and length, suggesting that they may contribute to the functional differences between IFITM family members (Jia et al. 2012, 2015).

The physical association of IFITM proteins was first described by John et al. (2013). They co-immunoprecipitated HA-tagged IFITM1, IFITM2 and IFITM3 together with untagged IFITM3 and suggested a model of IFITM3-mediated viral restriction based on intermolecular interactions that can change the fluidity of the host cell membrane. However, they were not able to solubilize the recombinant full-length IFITM3 protein and thus could not test for direct interaction. Zhao et al. (2014) suggested that IFITM1 protein may form heterooligomers with IFITM2 and/or IFITM3 and that this interaction suppresses their functions. In support of this hypothesis, they co-immunoprecipitated IFITM1 with IFITM2 and IFITM3. These findings point to the notion that the oligomerization of IFITM is important for its function, however, the structure of IFITM remains unknown. In this report, we define the molecular properties of IFITM1 by purifying the protein from bacterial expression systems. During this process, we discovered that the IFITM1 protein assembles into three distinct quaternary states; a monomer, dimer, and oligomer. We present data showing that these assemblies are irreversible which further suggests that upon protein synthesis, at least in bacterial expression systems, IFITM1 folds through different intrinsic protein folding pathways. If similar oligomeric assemblies are also present in human cells, it is critical to understand the mechanism by which IFITM1 oligomerizes and what is the physiological relevance of this phenomenon.

2 Results

2.1 Recombinant IFITM1 protein assembles into stable oligomers

To determine the biophysical characteristics of recombinant IFITM1, we purified full-length protein with His_6-tag on C-terminus (131 amino acids) using Immobilized Metal Affinity Chromatography (IMAC). During all purification steps, we utilized detergents as a measure of stabilizing the protein outside of its native environment. IFITM1 was successfully extracted from the membrane fraction using SDS as a primary detergent, which was subsequently exchanged on column during the IMAC purification, for DPC (or other detergents as mentioned in the Experimental procedures section). IMAC purification allowed us to obtain a protein sample of high purity as shown by SDS-PAGE analysis (Figure 1C, bottom panel, lane 1). Next, the IMAC-purified IFITM1 was concentrated and applied to size exclusion chromatography (SEC) column to assess the molecular weight of the eluted sample based on its retention volume (Figure 1C, top panel). We found that IFITM1 protein does not exist solely as a monomer; the SEC elution profile was broad with three distinct peaks: Species I (57–67 ml) marked in green, Species II (71–77 ml) marked in blue and Species III (81–87 ml) marked in red. The apparent mass of eluted species was spread between 300 and 17 kDa, according to the molecular weight (MW) standard. SDS-PAGE analysis of SEC fractions revealed that all of them contained IFITM1, suggesting the presence of different oligomeric states of IFITM1 (Figure 1C, bottom panel), which was confirmed with MS analysis (Supplementary Figure 1). The MS analysis has shown a different pattern of trypsin cleavage when comparing Species I and Species III to Species II.

To determine whether these oligomeric species are stable or revert in equilibrium to different oligomeric states, we isolated above mentioned fractions, concentrated each species identified in first SEC and re-applied them to SEC (Figure 1D, top panel). We observed that all the isolated species eluted at the same retention volume as it was during the first SEC analysis. We did not observe the collapse of isolated species into three distinct peaks as it was during the first analysis. This suggests that IFITM1 forms stable, distinct oligomeric species. Presumably, the polypeptide sequence follows different protein folding and assembly pathways during protein synthesis in the bacterial expression system that is reflected in these stable species. According to the MW standard the sample eluting at the lowest retention volume, which now we call “oligomer” (dotted green line), had a mass of more than 158 kDa. This sample contained SDS stable multimers (between 35 and 55 kDa) as well as the IFITM1 monomers (Figure 1D, bottom panel, lanes 1–2). The fractions derived from the middle peak, which were the most abundant isolated oligomeric species, now called “dimer” (dashed blue line), had a molecular weight of about 44 kDa based on the MW standard and also contained SDS stable oligomers with molecular weight between 25 and 35 kDa (Figure 1D, lanes 3–4). The fractions derived from the peak corresponding to the highest retention volume, now called “monomer” (red line), had a mass corresponding to approximately 17 kDa. SDS-PAGE analysis revealed that these fractions contained very little SDS stable oligomers and were largely monomeric (Figure 1D, lanes 5–6).

Dynamic light scattering (DLS) analysis of purified IFITM1 species showed homogenous, monodisperse populations for each oligomeric species (Figure 2A). Intensity size distribution plot shows a distinct shift in size between the species with a diameter of 10.1 nm for the oligomer, 7.5 nm for dimer and 5.6 nm for monomer.

Due to the low resolution of the DLS method and the inability to distinguish between the mass of the protein and

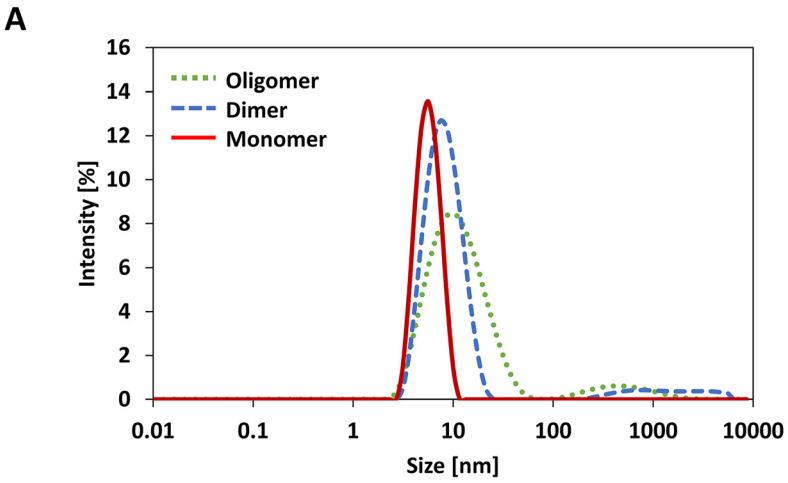

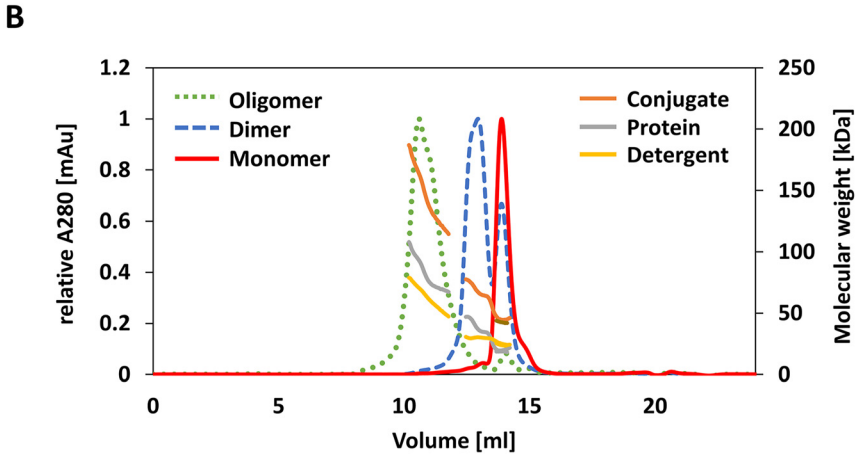

	MW (kDa) Conjugate (protein + detergent)	MW (kDa) protein	MW (kDa) detergent
Oligomer	147.8 (±0.6%)	83.4 (±0.6%)	64.4 (±1.4%)
Dimer	70.2 (±0.7%)	40.1 (±0.7%)	30.1 (±1.8%)
Monomer	42.6 (±0.6%)	18.6 (±0.5%)	24.0 (±1.1%)

Figure 2: IFITM1 protein exists as a monomer, dimer and larger oligomeric species.
(A) Dynamic Light Scattering results showing the intensity distribution of IFITM1 oligomeric species. (B) Multi-angle light scattering analysis showing the contribution of protein and detergent to molecular weight of IFITM1 oligomeric conjugates.

detergent in the conjugate (protein and detergent micelle), we decided to use additional methods to characterize the size of isolated IFITM1 oligomeric species. Multi-angle light scattering coupled with size exclusion chromatography (SEC-MALS) was used as a tool to determine the composition, mass, and oligomeric state of IFITM1 species. Measurement of absorbance at 280 nm enabled estimation of the protein concentration, while the multi-angle light scattering and refractive index detectors facilitated the calculation of the molecular weight and oligomeric state of the membrane protein as well as of the conjugate. The analysis was performed in the presence of 3 mM DPC. Conjugates of oligomer, dimer and monomer eluted as species of 147.8, 70.2 and 42.6 kDa, respectively. The molecular weight of the protein alone for the oligomer, dimer and monomer was 83.4, 40.1, and 18.6 kDa (Figure 2B). These data suggest that the oligomer is a tetrameric species. We observed slight contamination of dimer fraction with a monomeric form of IFITM1, however, it did not influence the calculation of its mass as the analysis revealed two distinct plateaus in mass

distribution across both peaks. As expected, the mass contribution of the detergent to each species was different. For the oligomer, after subtracting the mass of the protein from the conjugate we are left with 64.4 kDa corresponding to the detergent micelle. For the dimer, the mass is 30.1 kDa and for the monomer it is 24 kDa. These results are in line with the fact that the larger the protein size (the bigger the oligomer) the larger the amount of the detergent necessary for creating a membrane native-like environment.

Together, these data suggest that IFITM1 protein has a propensity to assemble into stable oligomeric species (likely dimeric and/or tetrameric), that can be isolated based on their oligomeric state.

To further evaluate the stability of the isolated oligomeric species, the purified fractions (from Figure 1D) were analyzed using gel electrophoresis without and with DTT and at room temperature or 95 °C (Figure 3A). Interestingly, the dimeric species were DTT-sensitive, suggesting a covalent bond forming the dimer, whilst the oligomer was DTT-resistant. A dynamic nature of the dimer was also suggested by CD thermal denaturation, where only the dimeric form of IFITM1 exhibits noticeable unfolding properties (Figure 3B).

2.2 ELISA experiments indicate the existence of putative structural motif within the N-terminus of IFITM1 protein which may be significant in oligomer formation

The sandwich ELISA is a method that can be used to determine the homo-oligomeric nature of a protein. We have previously characterized three monoclonal antibodies named MHK, TIL and STV covering three different epitopes in the N-terminus of IFITM1 (Figure 4A). MHK antibody recognizes IFITM1 and IFITM3 under both native and denaturing conditions (Gómez-Herranz et al. 2019) TIL antibody is specific to IFITM1 in its native conformation and STV binds only fully denatured recombinant IFITM1 protein (Supplementary Figure 2A–C). We used these reagents in sandwich ELISA to determine whether the oligomeric species exhibited evidence of 'dimerization'. The expectation is that if an epitope on the IFITM1 protein is occupied by a capture antibody, the protein cannot be detected by the same HRP-labeled detection antibody. If the protein forms a dimer or oligomer, it contains multiple epitopes, some of which may thus be free for binding of HRP-labeled detection antibody.

In a direct ELISA, MHK and TIL antibodies recognized all three IFITM1 species with similar intensity (Figure 4B and C). The STV antibody was used as a negative control

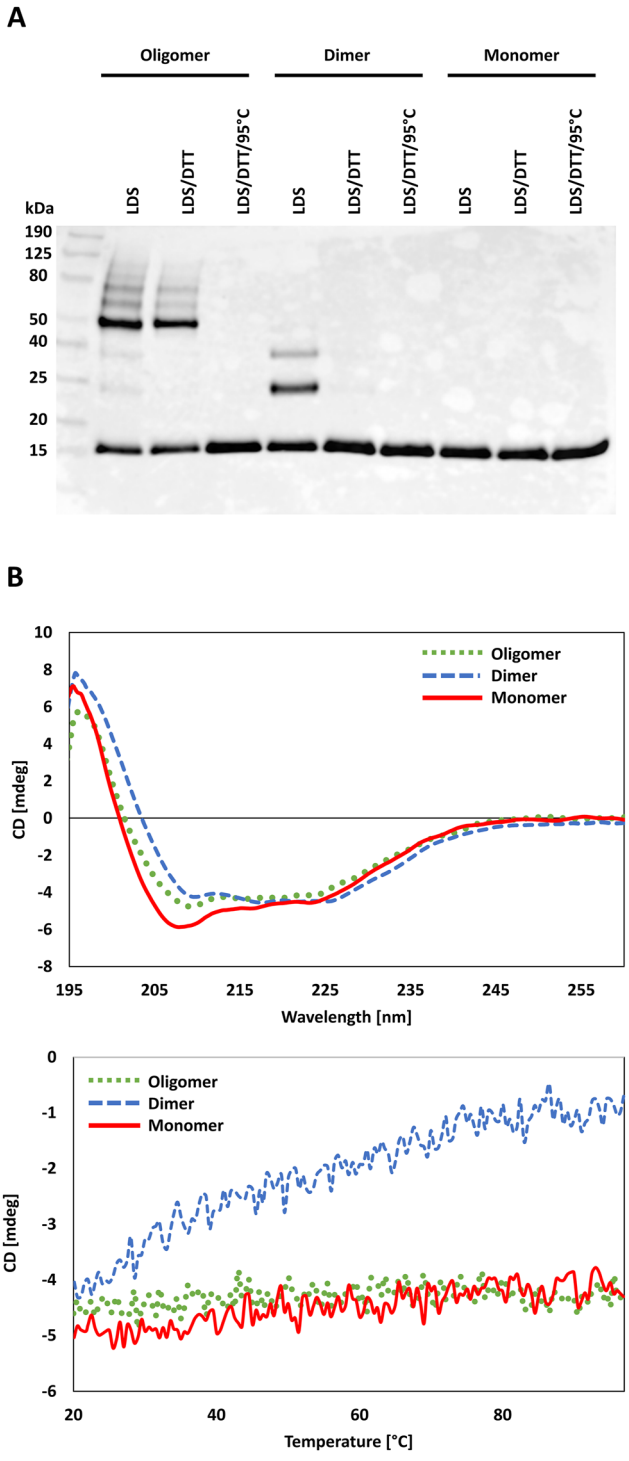

Figure 3: Different stability and secondary structure features of IFITM1 oligomeric species. (A) Purified proteins were mixed with LDS with or without DTT and incubated at 95 °C or at room temperature. Dimer form was sensitive to DTT reducing agent when compared to the oligomer. (B) Circular dichroism spectroscopy in the ultraviolet wavelength region (UV-CD) of IFITM1 species (left panel). Unfolding of IFITM1 species as a function of temperature at 220 nm (right panel).

(Supplementary Figure 3A). In the sandwich ELISA (Figure 5A–D), the MHK antibody did not detect any homo-oligomers when the MHK captured IFITM1 protein was challenged with MHK-HRP conjugated antibody (Figure 5A). As a control, the MHK captured IFITM1 protein could be detected after exposure to TIL-HRP conjugated antibody (Figure 5B). However, unlike the direct ELISA where the TIL-HRP binding was similar to all three IFITM1 forms, this was more pronounced on the dimeric and oligomeric species (Figure 5B, dotted green line and dashed blue line) than on the monomer (Figure 5B, red line). This further suggests either some steric constraints of the monomeric IFITM1 MHK epitope in the

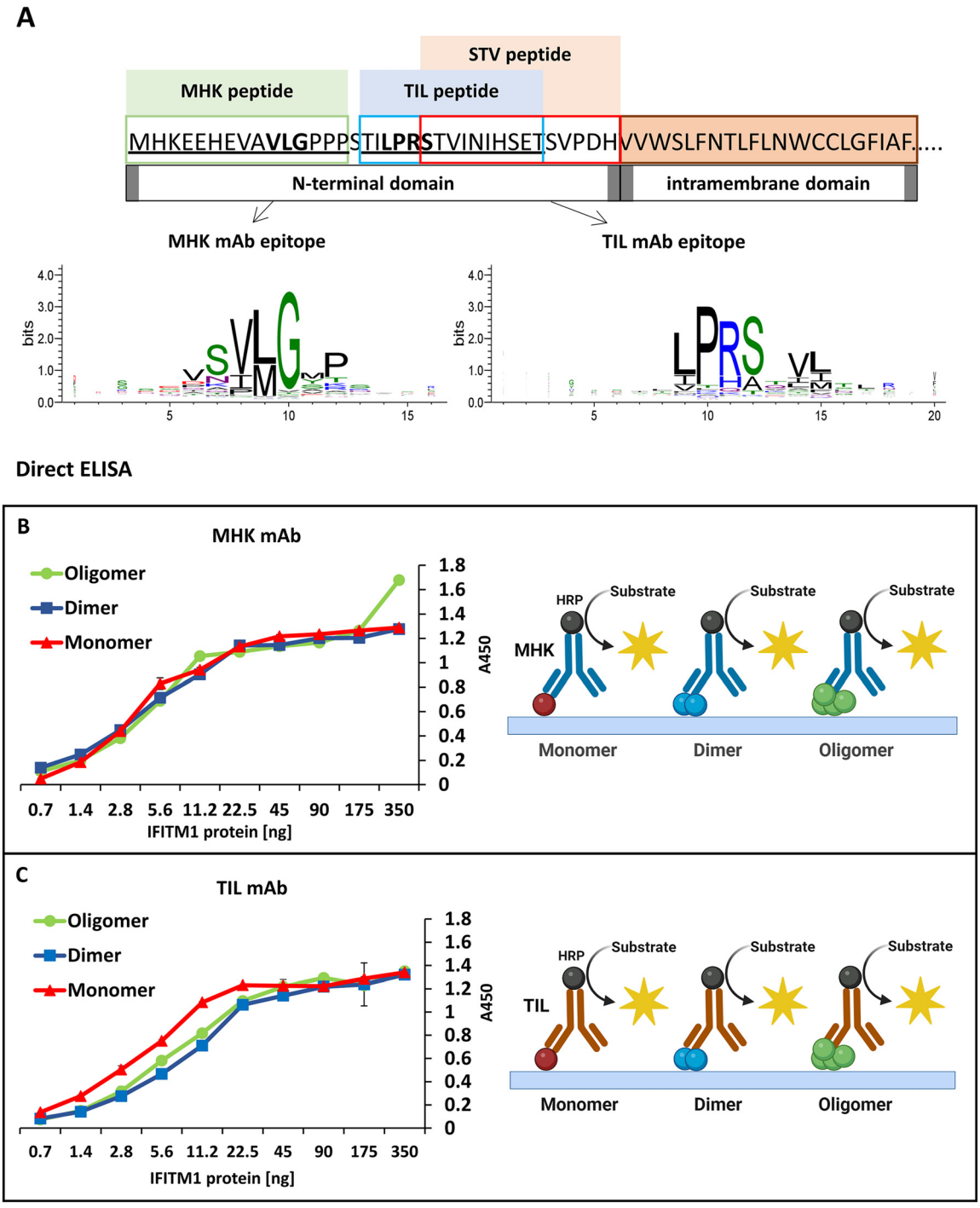

Figure 4: Direct ELISA for detection of IFITM1 oligomeric species. (A) Binding of HRP-labelled MHK antibodies to immobilized IFITM1 recombinant protein. (B) Binding of HRP-labelled TIL antibodies to immobilized recombinant proteins.

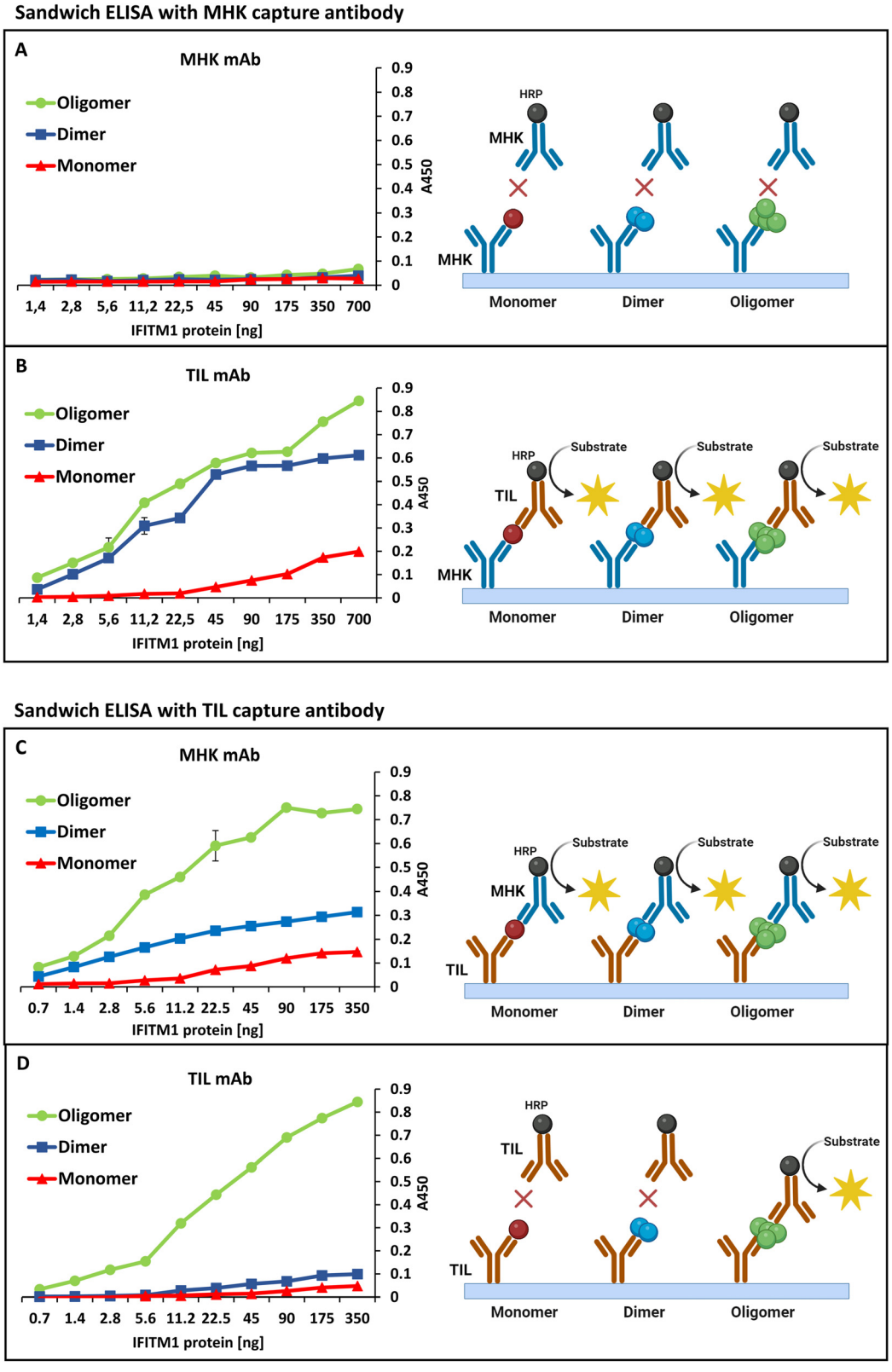

Figure 5: Sandwich ELISA for detection of IFITM1 oligomeric species. (A) IFITM1 recombinant protein is captured with MHK antibody and detected with HRP-labelled MHK or (B) TIL monoclonal antibodies. (C) IFITM1 recombinant protein is captured with TIL antibody and detected with HRP-labelled MHK or (D) TIL monoclonal antibodies.

ELISA configuration and that when dimeric or oligomeric, the TIL epitope can better detect the MHK captured IFITM1.

By contrast to the MHK epitope, evidence for oligomerization was identified using the TIL antibody. First, as a positive control, the TIL captured IFITM1 protein showed progressively increasing reactivity to the MHK-HRP conjugated antibody when analyzed on the monomer, dimer, and oligomer (Figure 5C, red, dashed blue, and dotted green line, respectively) compared to direct ELISA. This progressive increase might reflect that there are more epitopes on each IFITM1 species (i.e., 1, 2, and "4") that would lead to more mass being captured and a higher TMB signal.

When TIL was used to capture IFITM1, and then challenged with the TIL-HRP conjugated antibody, the oligomer species was detected (Figure 5D, dotted green line). However, the fact that the dimer was not detected using TIL capture and TIL-HRP challenge (Figure 5D, dashed blue line) further suggests a steric or conformational block using this combination of antibodies. STV antibody was used as a negative control (Supplementary Figure 3B and C).

2.3 HDX mass spectrometry defines the region responsible for assembly into higher-order structures

To determine which domains of IFITM1 are responsible for assembly into oligomeric species we used HDX mass spectrometry. In order to increase peptide identification, we tested several detergents that are compatible with this method. Two of them, mainly Octyl-beta-Glucoside and Deoxy Big Chap, have proven to be efficient in the stabilization of IFITM1 protein.

Peptide coverage was not uniform over the entire length of the protein sequence, peptic peptide fragments were largely mapped to amino acids in the intracellular NTD (1–36) and less in the CIL (58–86) and extracellular CTD (108–131) with the lowest peptic peptide recovery from amino acids in the membrane domains IMD (37–57) and TMD (87–107) and their surrounding regions (37–57 and 71–92) (Figure 6). The peptide mapping resulted in 143 unique IFITM1 peptides being identified and 100 % coverage of the protein sequence. However, hydrophobic regions were not easily accessible to pepsin cleavage and were therefore covered only by long peptides (Figure 6) which affects the accuracy of the measurement. The Deoxy Big Chap was finally used for HDX measurement due to the higher number of unique peptides identified compared to Octyl-beta-Glucoside (85 vs. 75).

In the presence of Deoxy Big Chap, there is progressive, but differential, deuterium suppression mainly from amino acids 25–41 and 59–70, less from 41–58 and 105–131 (Figure 7). In the 300 s time point, only oligomer was suppressed in these regions (Figure 7A, dotted green line). In the 1800 s time point, also dimer was suppressed, but less compared to oligomer (Figure 7B, dotted green and dashed blue lines). The region from amino acids 25–58 in the oligomer was equivalently suppressed in the 300 s and 1800 s time points (Figure 7A and B, dotted green line). By contrast, the region from amino acids 59–70 in the oligomer was suppressed more in the 1800 s time point and was extended by seven residues to amino acid 77 (Figure 7A and B, dotted green line).

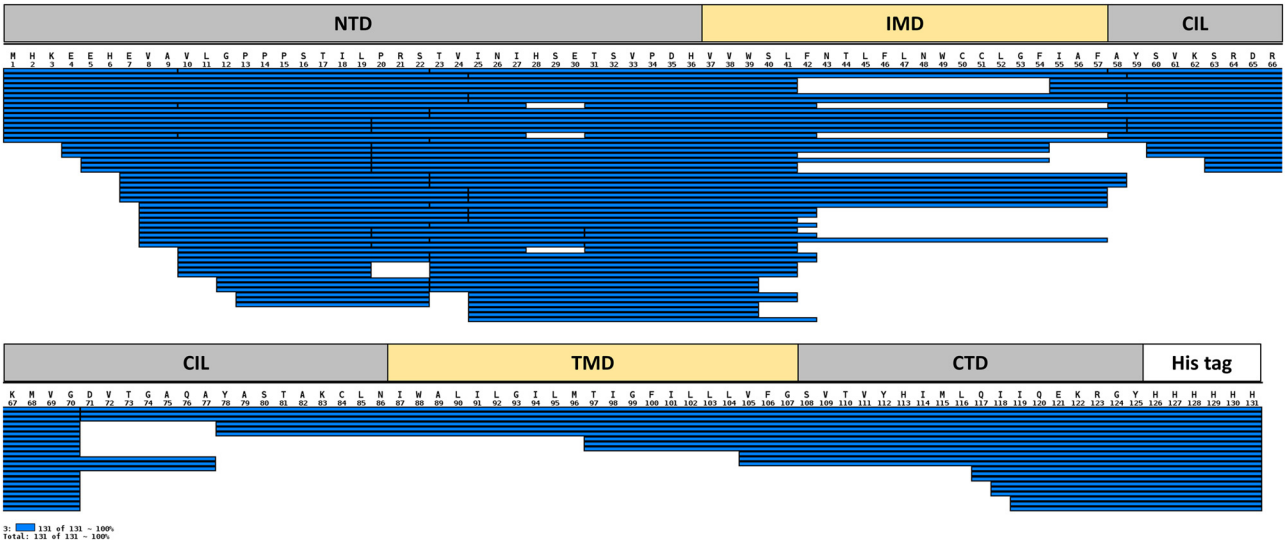

Figure 6: IFTM1 sequence coverage map. The mapping of peptic peptide fragments coverage of IFITM1 amino acid sequence using MSTools software. Blue boxes indicate the peptides common for all oligomeric states used for evaluation of deuterium uptake. The intracellular (NTD, CIL) and extracellular (CTD) IFITM1 domains are highlighted in gray, hydrophobic membrane regions (TMD, IMD) in yellow.

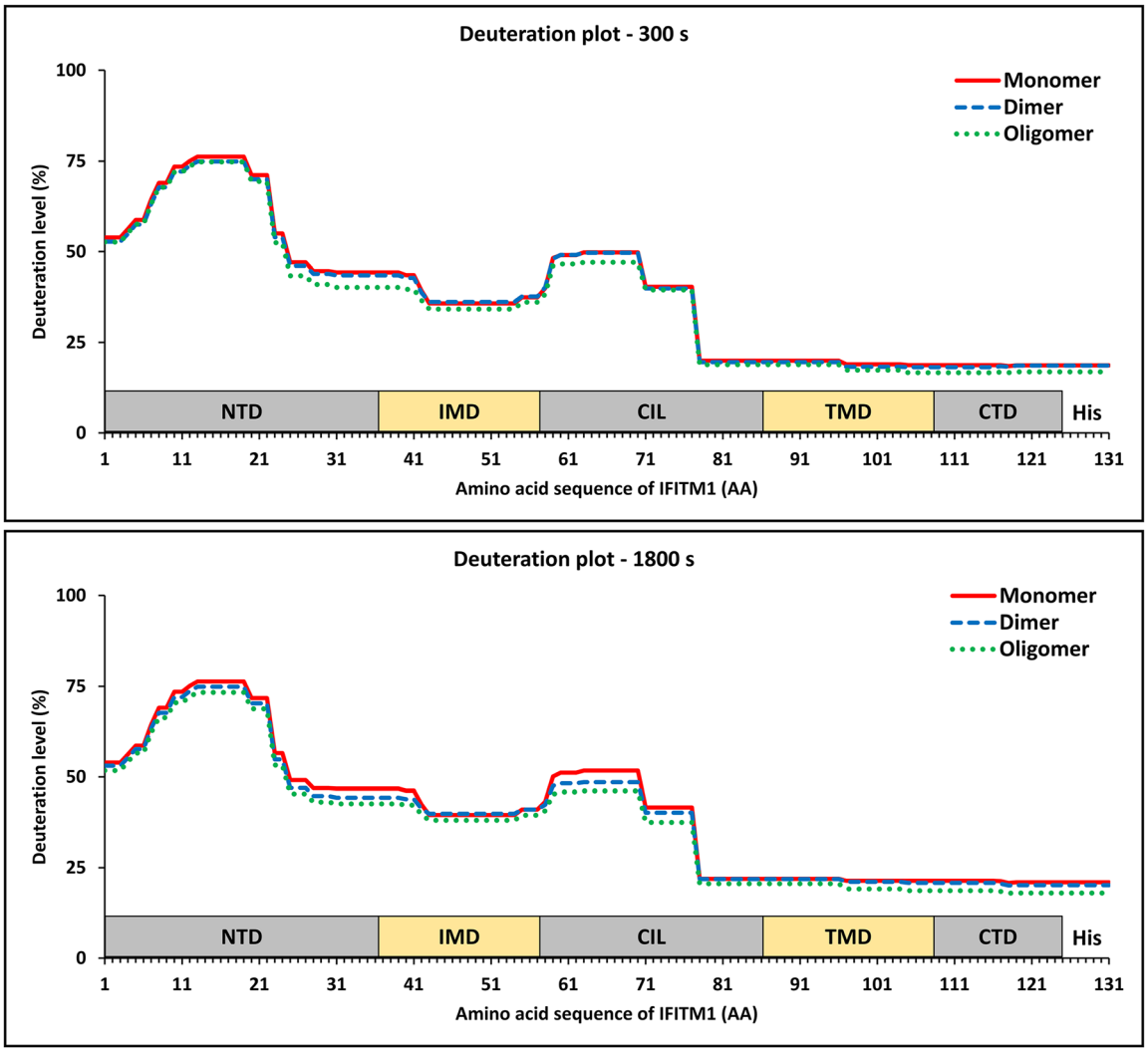

Figure 7: HDX analysis of IFITM1 oligomeric species. Comparison of structural properties of IFTM1 at different oligomeric self-association states. Similarity of IFITM1 at monomeric (red line), dimeric (dashed blue line), and oligomeric (dotted green line) states as mean % deuterium uptake for each amino acid after (A) 300 s and (B) 1800 s deuteration. The intracellular (NTD, CIL) and extracellular (CTD) IFITM1 domains are highlighted in gray, hydrophobic membrane regions (TMD, IMD) in yellow.

Together, these data suggest that the oligomeric nature of IFITM1 extends throughout a large proportion of the protein, mainly at the interface of NTD and IMD and in the CIL.

3 Discussion

Oligomerization is a common property of proteins. It is estimated that at least 35 % of all proteins in cells are oligomeric (Goodsell and Olson 2000; Jones and Thornton 1996). Some proteins form one specific active oligomeric state, others are in equilibrium between different oligomeric forms and regulation of this equilibrium plays a central role in maintaining their activity and function (Gabizon and Friedler 2014). Development of molecules that bind preferentially to a specific oligomeric state and modulate the oligomerization equilibrium is emerging as a potential therapeutic strategy for cancer and viral infections.

IFITM1, is a key player in the cell antiviral response and also has the ability to oligomerize. Homo- and hetero-oligomerization of IFITM family members was previously described in cell lysates (John et al. 2013; Zhao et al. 2014). Here, we show for the first time oligomerization of purified IFITM1 protein *in vitro*. It is important to mention the weakness of the bacterial expression system that it is often not able to produce a recombinant human protein identical to the naturally occurring wild type. Bacteria lack sophisticated mechanisms for performing posttranslational modifications which are present in eukaryotic cells. IFITMs are also regulated by several post-translational modifications that include

ubiquitination, methylation, palmitoylation and phosphorylation (Chesarino et al. 2014; Friedlova et al. 2022). These modifications determine the intracellular localization and antiviral activity of IFITMs, but their effect on oligomer formation has not yet been studied. According to findings on other oligomer-forming proteins, the oligomerization is affected more often by ligand binding or domain swapping and the effect of post-translational modifications was shown to influence protein oligomerization/aggregation mainly in neurodegenerative diseases (Kumari and Yadav 2019; Schaffert and Carter 2020). Nevertheless, we cannot exclude their impact on IFITM1 oligomerization.

Expression and purification of membrane proteins for structural purposes are even more challenging because it is necessary to mimic their native environment to get correctly folded proteins. There are several methods how to preserve the native conformation of membrane proteins. The most common way is to use detergents or lipid membrane mimics such as nano-discs (Errasti-Murugarren et al. 2021). In this work, full-length IFITM1 protein with a C-terminal His-tag was successfully purified from the membrane fraction and further stabilized with DPC detergent. Subsequent SEC analysis showed an elution profile with three distinct peaks of different molecular weight. We assumed that these could be stable IFITM1 oligomeric species or they might revert in equilibrium to different oligomeric states. SEC re-analysis showed that these species are stable, and we called them monomer, dimer and oligomer according to their estimated molecular weight. To further characterize isolated oligomeric species, the SEC-MALS method was used. Conjugates of protein with detergent micelles were eluted and molecular weights of different species and mass contribution of the detergent were calculated, whereby we can propose a monomeric, dimeric, and tetrameric structure to the species.

The stability of IFITM1 oligomeric species was tested using reducing agents (DTT), high temperature and detergents. In general, the oligomer and dimer were not collapsed into monomers regardless of SDS concentration. Interestingly, the dimer, but not oligomer, was shown to be sensitive to DTT reduction. The different stability of the oligomeric species was confirmed by CD spectroscopy, where only dimeric form of IFITM1 exhibits unfolding during thermal denaturation. We cannot explain this based on the other orthogonal data in this study (i.e., sandwich ELISA and HDX mass spectrometry), however, it further suggests a dynamic conformational state of IFITM1. Future studies might show its impact on heterologous protein interactions or equilibrium with its membrane insertion.

A sandwich ELISA was used as an orthogonal method to determine whether we could detect homo-oligomers of IFITM1 based on the assumption that if an epitope on a protein is occupied by a capture antibody, that same HRP-labelled antibody can only detect that protein if it forms a dimer or oligomer that provides additional free epitopes. Only the oligomer form of IFITM1 exhibited pronounced evidence of oligomerization using antibody that binds the conformational epitope within the NTD. However, only the TIL/TIL-HRP antibody combination, rather than the MHK/MHK-HRP antibody combination could detect this oligomerization. It is conceivable that the binding of the MHK antibody to the N-terminus disrupts the oligomerization so that there are no oligomers captured using the MHK/MHK-HRP antibody combination. It would be interesting to examine in the future if IFITM1-binding proteins that interact at this extreme N-terminus could also regulate oligomerization. These data suggest that the dimer and oligomer are relatively distinct which is consistent with the DTT-sensitivity of the dimeric species. In summary, ELISA confirmed oligomerization of IFITM1 *in vitro*, however, only under certain conditions. The different behavior of MHK and TIL antibodies suggests the existence of some structural motif within the N-terminus of IFITM1 protein which may be significant in oligomer formation.

To localize regions in the IFITM1 that are important for the assembly of oligomers, IFITM1 oligomeric species were analyzed with HDX mass spectrometry. The peptide mapping correlated with the predicted domain structure – more peptides were identified from hydrophilic regions (mainly from extracellular CTD and also intracellular NTD and CIL), less from hydrophobic regions (IMD and TMD). After optimization of purification process with MS-compatible detergents, the sequence coverage was 100 %. The progressive deuterium suppression, which is related to the site of assembly, was detected mainly in the N-terminal part of the protein, specifically in amino acid regions 25–41 and 59–70 (77) and less from 41–58 and 105–131. The most suppressed regions contain parts of NTD, IMD and CIL. The CTD showed only small changes in deuteration. John et al. (John et al. 2013) described two phenylalanine residues within IMD (F75 and F78) as important for the physical interaction of the IFITM proteins. These amino acids were also shown to be necessary for antiviral activity of IFITM proteins (Chmielewska et al. 2022; John et al. 2013; Zhao et al. 2014) and John et al. (2013) suggested that oligomerization might be the key mechanism of IFITM protein mediated viral restriction because intermolecular interactions between IFITM proteins may change cell membrane properties (may decrease membrane fluidity, as well as alter the bending modulus of the endosomal membrane, increasing the force required by the viral fusion machinery to deform the membrane).

However, another study that used a flow cytometry-based fluorescence energy resonance transfer (FRET) approach later indicated that these phenylalanine residues are unnecessary

for oligomerization (Winkler et al. 2019). Based on the homology between the IFITM3 and PRRT2 proteins, Rahman et al. (Rahman et al. 2020) described a conserved 91GXXXG95 motif (homologous with 70GXXXG74 in IFITM1) as responsible for the oligomeric state, with both glycine residues participating in oligomerization and G95 having a stronger effect. The GXXXG motif belongs to the CIL and is typically involved in protein dimerization (Mueller et al. 2014; Rahman et al. 2020). Mutations in these glycine residues significantly decreased antiviral properties of IFITM3 by preventing membrane rigidification (Rahman et al. 2020). Studying the effect of mutations in these regions on the oligomerization of the IFITM1 protein *in vitro* will therefore be a logical continuation of this work. Overall, the growing knowledge on IFITM oligomeric variants suggests a crucial role for oligomerization in the regulation of IFITM functions.

Moreover, the level of overall deuteration should correlate with accessibility of amino acids to the solvent and thus can give us some information about the possible 3D structure of IFITM1. Interestingly, low deuteration of the very C-terminal part of the protein (78–131; less than 25 % overall) suggests that this region is relatively hidden compared to more deuterated N-terminal part (which exhibits ~50 % of overall deuteration; Figure 7). This C-terminal region is divided into two parts; (i) the region comprising amino acids 87–107 is predicted to be within a membrane space and is very hydrophobic (Figure 1A and B); and (ii) the C-terminal tail which is predicted to be solvent accessible and in the current model (Figure 1A), outside the cell. Although we can rationalize that amino acids 80–110 have a lowered deuteration level due to the fact that they are bound to the detergent micelle, the C-terminal tail should not have these same properties. This might suggest a cis (intramolecular) interaction site for amino acids 108–125 within the core of IFITM1 monomeric form that is independent of the trans (intermolecular) 25–41 and 59–70 (77) amino acid interaction sites in the oligomeric forms (Figure 7). On the contrary, the deuteration in the NTD ranges from 50 to 75 %. The region with the highest deuteration contains the epitope of TIL antibody that binds IFITM1 protein only in its native conformation and thus have some conformational epitope. However, this region is also dynamic in terms of its suppression of deuteration as a function of its oligomeric state.

Together, these data suggest that the oligomeric nature of IFITM1 is confined to a broad region in the N-terminal half of the protein, flanking the IMD and provides hypothesis for testing how it might oligomerize in cell membranes. A more detailed knowledge of the IFITM protein structure and oligomerization is of great importance because IFITMs are involved in antiviral immunity as well as in tumor progression.

4 Materials and methods

4.1 Protein expression and purification

The pET22b expression plasmid containing IFITM1 with C-terminal His_6-tag was transformed into *Escherichia coli* Rosetta™ 2 (DE3) pLysS cells (Novagen). Cells were grown in lysogeny broth (LB) medium supplemented with 100 µg/ml of ampicillin and 34 µg/ml of chloramphenicol at 37 °C to an OD_{600} = 0.6. Expression was induced by adding 1 mM isopropyl β-D-1-thiogalacto-pyranoside (IPTG) and protein was expressed for 16 h at 25 °C. Cells were harvested by centrifugation and resuspended in Lysis Buffer (70 mM Tris-HCl pH 8.0, 300 mM NaCl) with the addition of protease inhibitors (1 µM E–64, 0.75 µM Pepstatin A, 5 µM Leupeptin) and lysed by sonication. The membrane fraction was harvested by ultracentrifugation and solubilized in Binding Buffer (20 mM Tris-HCl pH 8.0, 200 mM NaCl, 1 % Sodium Dodecyl Sulphate (SDS), 20 mM β-mercaptoethanol) with the addition of protease inhibitors (1 µM E–64, 0.75 µM Pepstatin A, 5 µM Leupeptin) at room temperature for 4 h. After removal of unsolubilized material by ultracentrifugation supernatant was loaded onto the column with Protino® NiNTA agarose (Macherey-Nagel) equilibrated with Binding Buffer. Resin was washed with 10 column volumes of Wash Buffer 1 (20 mM Tris pH 8.0, 200 mM NaCl, 1 % SDS, 10 mM imidazole, 20 mM β-mercaptoethanol). Detergent was exchanged on column using Wash Buffer 2 (20 mM Tris pH 8.0, 200 mM NaCl, 0.5 % n-dodecylphosphocholine (DPC) (Avanti Lipids), 10 mM imidazole, 20 mM β-mercaptoethanol) and the protein was eluted with Wash Buffer two supplemented with 200 mM imidazole. Fractions were concentrated with centrifugal concentrator Vivaspin Turbo 4 with 10,000 MWCO (Sartorius) and during this step buffer was exchanged to Gel Filtration Buffer (20 mM Tris pH 8.0, 300 mM NaCl, 3 mM DPC, 2 mM TCEP, 5 % glycerol). Protein was loaded onto the gel filtration column (HiLoad 16/60 Superdex 200 pg, GE Healthcare or Superdex™ 200 10/300 GL, GE Healthcare).

4.2 Separation of IFITM1 oligomeric species

To separate different oligomeric species of IFITM1 protein, three peaks were collected (57–67 ml, 71–77 ml, 81–87 ml). Collected fractions were separately concentrated with centrifugal concentrator Vivaspin Turbo 4 with 10,000 MWCO (Sartorius) and re-applied on gel filtration. After each run fractions were collected, samples were concentrated with centrifugal concentrator Vivaspin Turbo 4 with 10,000 MWCO (Sartorius) to approximately 30 µM and stored at −80 °C for further assays. Protein purity was assessed by SDS-PAGE and concentration was estimated spectrophotometrically using extinction coefficient $\varepsilon_{280(monomer)}$ = 14,787 $M^{-1}\,cm^{-1}$.

4.3 Identification of IFITM1 oligomeric species with mass sepctrometry

Bands corresponding to IFITM1 oligomer, dimer and monomer were excised from the SDS-PAGE gel and sent for the analysis at the Mass Spectrometry Laboratory IBB PAS, Warsaw, by LC-MS-MS/MS (liquid chromatography coupled to tandem mass spectrometry) using NanoAcquity (Waters) LC system and LTQ-FT-Orbitrap mass spectrometer (Thermo Electron Corp., San Jose, CA). Resulting raw data were processed by Mascot Distiller, followed by Mascot Search (Matrix Science,

London, UK) against the Swiss-Prot database restricted to *H. sapiens* sequences.

4.4 Circular dichroism spectroscopy

CD spectra (195–260 nm) of IFITM1 protein at 2.5 µM concentration in buffer containing 140 mM KCl, 20 mM potassium phosphate pH 7.5 and 3 mM DPC were collected on Circular Dichroism Spectrometer Jasco J-1500 at 20 °C. Reported CD curve is an average of five scans, and it was corrected for the contribution of the buffer alone. Circular dichroism was also used to determine unfolding of protein as a function of temperature (20–97 °C), at a wavelength of 220 nm, to determine protein stability and melting temperature.

4.5 Dynamic light scattering (DLS)

The homogeneity of purified fractions was determined using Malvern Instruments ZetaSizer Nano S dynamic light scattering instrument. Measurements were taken in Gel Filtration Buffer (20 mM Tris pH 8.0, 300 mM NaCl, 3 mM DPC, 2 mM TCEP, 5 % glycerol) at 25 °C. Protein concentration for monomer and both oligomeric species was 30 µM and three measurements of 10 runs of 10 s each were averaged to obtain intensity size distribution of each particle.

4.6 Size exclusion chromatography coupled with multi-angle light scattering (SEC-MALS)

To determine the contribution of the protein and detergent to the molecular mass of conjugate MALS method was applied. The analysis was done using the SEC column (Superdex™ 200 10/300 GL, (GE Healthcare) coupled with UV detector, miniDAWN® (MALS detector) and Optilab® (differential refractometer) (Wyatt Technology). The analysis was performed in Gel Filtration Buffer (20 mM Tris pH 8.0, 300 mM NaCl, 3 mM DPC, 2 mM TCEP, 5 % glycerol) at 4 °C. The sample was thawed and filtered using a 0.22 µm spin filter to remove larger aggregates. 100 µg of purified proteins (monomer and both oligomeric species) was injected for separation and analysis. Data collection and SEC-MALS analysis were performed with ASTRA eight software (Wyatt Technology). *dn/dc* (refractive index increment) value for all samples was defined as 0.185 mL/g (a standard value for proteins) and *dn/dc* for detergent was 0.1398 mL/g.

4.7 IFITM1 monoclonal antibodies

Novel monoclonal antibodies targeting IFITM1 were developed by Moravian-Biotechnology (Czech Republic) from mice immunized with partially overlapping 15-mer peptides from IFITM1 protein; MHKEEHEVAVLGPPP, TILPRSTVINIHSET and STVINIHSETSVPDH (Clonestar, Czech Republic) from the N-terminal part of human IFITM1. The resulting hybridoma clones were tested for the ability of produced immunoglobulins to bind purified recombinant IFITM1 protein as well as endogenously expressed IFITM1. All three monoclonal antibodies named MHK, TIL and STV that were finally chosen for further experiments were able to bind denatured IFITM1-GST recombinant protein and MHK antibody, but not TIL or STV, recognized denatured endogenously expressed IFITM1 ((Gómez-Herranz et al. 2019), Supplementary Figure 2A and B). Immunoprecipitation proved that MHK and TIL antibodies, but not STV, bind also endogenous IFITM1 in its native conformation (Supplementary Figure 2C). Epitopes were mapped using peptide-phage display as described previously (Krejci et al. 2016) which highlights the consensus site of the key antibodies MHK and TIL (Figure 4A). The consensus site matches the actual sequence of the peptide immunogen and gives us confidence of the differences in both MHK and TIL epitopes.

4.8 Enzyme-linked immunosorbent assay (ELISA)

For direct ELISA, 96-well microtitration plates (Gama, V400920) were coated with 50 µl per well of IFITM1 proteins from different SEC fractions, diluted in coating buffer (0.1 M carbonate-bicarbonate, pH 9.5) overnight at 4 °C. Plates were blocked in blocking buffer (3 % immunoglobulin free BSA in PBS) for 2 h at RT, washed in washing buffer (PBS + 0.1 % NP-40) and incubated with HRP-labelled MHK, TIL and STV antibodies (1 µg/ml in 1 % BSA in PBS) for 2 h at RT. After washing three times in washing buffer, samples were incubated with tetramethylbenzidine (TMB) resuspended in 0.1 M citrate/phosphate buffer pH 6.0 with hydrogen peroxide for 30 min, the reaction was stopped with 1 M sulfuric acid and signal was measured at 450 nm with Tecan microplate reader.

For sandwich ELISA, plates were coated with MHK or TIL antibody (1 µg/ml in coating buffer) overnight at 4 °C, blocked in blocking buffer for 2 h at room temperature and incubated with IFITM1 proteins from three pooled fractions diluted in DPC buffer (20 mM Tris, pH 8.0; 30 mM NaCl; 3 mM n-dodecylphosphocholine; 5 % glycerol, 2 mM TCEP). HRP-labelled MHK, TIL and STV antibodies were used to detect the captured protein. Signal was developed as in direct ELISA.

4.9 SDS-PAGE and western blotting

In order to test the stability of purified proteins, 100 ng of each monomer and oligomeric species were mixed with NuPAGE LDS sample buffer (Thermo Fisher Scientific) and then were tested in the presence or absence of 0.1 M DTT both while heated to 95 °C for 5 min or at room temperature. Samples were loaded onto 10 % polyacrylamide gels and the protein separation was performed in MOPS running buffer (50 mM MOPS, 50 mM Tris Base, 0.1 % SDS, 1 mM EDTA, pH 7.7) for about 2 h at 120 V. Separated proteins were transferred onto nitrocellulose membranes (Bio Tech, PALL Corporation) 1 h at 100 V. Nonspecific binding was blocked using 5 % milk in PBS with 0.1 % Tween (PBST) for 45 min on an orbital shaker. The primary antibody mouse MHK was diluted in 5 % milk in PBST and incubated with the membranes overnight at 4 °C. Membranes were then washed three times in PBST and incubated with the horseradish peroxidase (HRP)-conjugated rabbit anti-mouse secondary antibody (Dako) diluted in 5 % milk in PBST for 1 h at room temperature. Membranes were washed again in PBST three times and proteins were visualized with enhanced chemiluminescence (ECL) reagent and GeneTools (Syngene).

4.10 Hydrogen/deuterium exchange (HDX) mass spectrometry

For HDX experiments C-terminally His_6-tag fused IFITM1 was purified as described above only instead of DPC, Octyl-beta-Glucoside or Deoxy Big Chap detergents were used, with their final concentrations in the Gel Filtration Buffer of 25 mM and 1.5 mM respectively. Samples containing

IFITM1 monomer, dimer or oligomer were diluted with buffer (20 mM Tris-HCl pH 8.0; 300 mM NaCl, 1 mM TCEP) in H_2O to prepare undeuterated controls and for peptide mapping, or with the buffer in D_2O (20 mM Tris-HCl pH 7.6, 300 mM NaCl, 1 mM TCEP) to prepare deuterated samples. The final concentrations of the protein samples used for analysis was 3 µM. Hydrogen-deuterium exchange was carried out at room temperature and was quenched after 5 min or 30 min by adding 0.875 M HCl in 1 M glycine with pepsin followed with 3 min incubation and rapid freezing in liquid nitrogen. Each sample was thawed and injected into an LC-system (UltiMate 3000 RSLCnano, Thermo Scientific) with an immobilized Nepenthesin-1 enzymatic column 15 µl bed volume (Affipro s.r.o., CZ) flow rate 50 µl/min, 2 % acetonitrile/0.05 % trifluoroacetic acid. Peptides were trapped and desalted online on a peptide microtrap (Michrom Bioresources) for 3 min at a flow rate of 50 µl/min. Next, the peptides were eluted onto an analytical column (Jupiter C18, 1.0 × 50 mm, 5 µm, 300 Å, Phenomenex) and separated by linear gradient elution starting with 10 % buffer B in buffer A and rising to 65 % buffer B over 30 min at a flow rate of 20 µl/min. Buffers A and B consisted of 0.1 % formic acid in water and 80 % acetonitrile/0.08 % formic acid, respectively. The immobilized Nepenthesin-1 column, trap cartridge, and analytical column were kept at 1 °C.

Mass spectrometric analysis was carried out using an Orbitrap Elite mass spectrometer (Thermo Fisher Scientific) with ESI ionization connected online to a robotic system based on the HTS-XT platform (CTC Analytics). The instrument was operated in a data-dependent mode for peptide mapping (HPLC-MS/MS). Each MS scan was followed by MS/MS scans of the three most intensive ions from both CID and HCD fragmentation spectra. Tandem mass spectra were searched using SequestHT against the cRap protein database (ftp://ftp.thegpm.org/fasta/cRAP) containing the sequence of IFITM1 with the following search settings: mass tolerance for precursor ions of 10 ppm, mass tolerance for fragment ions of 0.6 Da, no enzyme specificity, two maximum missed cleavage sites and no-fixed or variable modifications. The false discovery rate at the peptide identification level was set to 1 %. Sequence coverage was analyzed with Proteome Discoverer version 1.4 (Thermo Fisher Scientific) and graphically visualized with the MS Tools application1. Analysis of deuterated samples was done in HPLC-LC-MS mode with ion detection in the orbital ion trap. The MS raw files together with the list of peptides (peptide pool) identified with high confidence characterized by requested parameters (amino acid sequence of each peptide, its retention time, XCorr, and ion charge) were processed using HDExaminer version 2.2 (Sierra Analytics). The software analyzed protein and peptides behaviour, created the uptake plots that showed peptide deuteration over time with calculated confidence level (high, medium confidence are accepted, low confidence is rejected). All peptides with assigned confidence were considered to map uptake values to each of the protein residues. Each residue was annotated with as many deuteration values as peptides mapped to that particular residue by calculation of the individual amino acids (expressed as percentage of deuteration) corresponding to the average of all deuteration values assigned (Smit et al. 2021; Nemergut et al. 2023; Stofella et al. 2022). The mass spectrometry proteomics data have been deposited to the ProteomeXchange Consortium via the PRIDE2 partner repository with the dataset identifier PXD029724; Username: reviewer_pxd029724@ebi.ac.uk, Password: g9W0wNk8.

Acknowledgments: We thank Dr. Christian Sieg from Wyatt Technology for help with SECMALS data collection and analysis.

Research ethics: The local Institutional Review Board deemed the study exempt from review.

Author contributions: MN and MW designed and carried out the experiments, prepared figures and wrote the manuscript (they contributed equally). NF, LU and VH carried out the experiments. FZK analyzed the data. LH, BV, TRH and MRS did supervision of work, contributed to experimental design and writing and revised the manuscript. All authors have accepted responsibility for the entire content of this manuscript and approved its submission.

Competing interests: BV is a consultant for Moravian Biotechnology, who supplied the MHK, TIL and STV antibodies used in this study. The company had no role in the design, execution, interpretation or writing of the study. All other authors state no conflict of interest.

Research funding: This work was supported with Czech Science Foundation (GACR) 22-02940S, MH CZ – DRO (MMCI, 00209805); the BBSRC RASOR consortium (BB/C511599/1; United Kingdom); The First TEAM program cofinanced by Foundation for Polish Science and European Union under the European Regional Development Fund (POIR.04.04.00-00-3E44/17-00). The International Centre for Cancer Vaccine Science project carried out within the International Research Agendas programme of the Foundation for Polish Science co-financed by the European Union under the European Regional Development Fund. This work was supported by the Ministry of Education and Science, Poland and the EMBO Installation Grant (4129).

Data availability: The raw data can be obtained on request from the corresponding author.

References

Bailey, C.C., Zhong, G., Huang, I.-C., and Farzan, M. (2014). IFITM-family proteins: the cell's first line of antiviral defense. *Annu. Rev. Virol.* 1: 261–283.

Brass, A.L., Huang, I.-C., Benita, Y., John, S.P., Krishnan, M.N., Feeley, E.M., Ryan, B.J., Weyer, J.L., Van Der Weyden, L., Fikrig, E., et al. (2009). The IFITM proteins mediate cellular resistance to influenza A H1N1 virus, west nile virus, and dengue virus. *Cell* 139: 1243–1254.

Chesarino, N.M., McMichael, T.M., and Yount, J.S. (2014). Regulation of the trafficking and antiviral activity of IFITM3 by post-translational modifications. *Future Microbiol.* 9: 1151–1163.

Chmielewska, A.M., Gómez-Herranz, M., Gach, P., Nekulova, M., Bagnucka, M.A., Lipińska, A.D., Rychłowski, M., Hoffmann, W., Król, E., Vojtesek, B., et al. (2022). The role of IFITM proteins in tick-borne encephalitis virus infection. *J. Virol.* 96: e01130-21.

Diamond, M.S. and Farzan, M. (2013). The broad-spectrum antiviral functions of IFIT and IFITM proteins. *Nat. Rev. Immunol*. 13: 46–57.

Errasti-Murugarren, E., Bartoccioni, P., and Palacín, M. (2021). Membrane protein stabilization strategies for structural and functional studies. *Membranes (Basel)* 11: 155.

Friedlová, N., Zavadil Kokáš, F., Hupp, T.R., Vojtěšek, B., and Nekulová, M. (2022). IFITM protein regulation and functions: far beyond the fight against viruses. *Front. Immunol.* 13: 1042368.

Friedman, R.L., Manly, S.P., McMahon, M., Kerr, I.M., and Stark, G.R. (1984). Transcriptional and posttranscriptional regulation of interferon-induced gene expression in human cells. *Cell* 38: 745–755.

Gabizon, R. and Friedler, A. (2014). Allosteric modulation of protein oligomerization: an emerging approach to drug design. *Front. Chem.* 2: 9.

Gómez-Herranz, M., Nekulova, M., Faktor, J., Hernychova, L., Kote, S., Sinclair, E.H., Nenutil, R., Vojtesek, B., Ball, K.L., and Hupp, T.R. (2019). The effects of IFITM1 and IFITM3 gene deletion on IFNγ stimulated protein synthesis. *Cell Signalling.* 60: 39–56.

Goodsell, D.S. and Olson, A.J. (2000). Structural symmetry and protein function. *Annu. Rev. Biophys. Biomol. Struct*. 29: 105–153.

Jia, R., Ding, S., Pan, Q., Liu, S.-L., Qiao, W., and Liang, C. (2015). The C-terminal sequence of IFITM1 regulates its anti-HIV-1 activity. *PLoS ONE* 10: e0118794.

Jia, R., Pan, Q., Ding, S., Rong, L., Liu, S.-L., Geng, Y., Qiao, W., and Liang, C. (2012). The N-terminal region of IFITM3 modulates its antiviral activity by regulating IFITM3 cellular localization. *J. Virol*. 86: 13697–13707.

John, S.P., Chin, C.R., Perreira, J.M., Feeley, E.M., Aker, A.M., Savidis, G., Smith, S.E., Elia, A.E.H., Everitt, A.R., Vora, M., et al. (2013). The CD225 domain of IFITM3 is required for both IFITM protein association and inhibition of influenza A virus and dengue virus replication. *J. Virol*. 87: 7837–7852.

Jones, S. and Thornton, J.M. (1996). Principles of protein-protein interactions. *Proc. Natl. Acad. Sci. U.S.A.* 93: 13–20.

Krejci, A., Hupp, T.R., Lexa, M., Vojtesek, B., and Muller, P. (2016). Hammock: a hidden Markov model-based peptide clustering algorithm to identify protein-interaction consensus motifs in large datasets. *Bioinformatics* 32: 9–16.

Kumari, N. and Yadav, S. (2019). Modulation of protein oligomerization: an overview. *Prog. Biophys. Mol. Biol.* 149: 99–113.

Lange, U., Saitou, M., Western, P., Barton, S., and Surani, M. (2003). The Fragilis interferon-inducible gene family of transmembrane proteins is associated with germ cell specification in mice. *BMC Dev Biol* 3: 1.

Liang, R., Li, X., and Zhu, X. (2020). Deciphering the roles of IFITM1 in tumors. *Mol Diagn Ther* 24: 433–441.

Mueller, B.K., Subramaniam, S., and Senes, A. (2014). A frequent, GxxxG-mediated, transmembrane association motif is optimized for the formation of interhelical Cα–H hydrogen bonds. *Proc. Natl. Acad. Sci. U.S.A.* 111: E888–E895.

Nemergut, M., Marques, S.M., Uhrik, L., Vanova, T., Nezvedova, M., Gadara, D.C., Jha, D., Tulis, J., Novakova, V., Planas-Iglesias, J., et al. (2023). Domino-like effect of C112R mutation on ApoE4 aggregation and its reduction by alzheimer's disease drug candidate. *Neuroscience* 18: 38.

Paysan-Lafosse, T., Blum, M., Chuguransky, S., Grego, T., Pinto, B.L., Salazar, G.A., Bileschi, M.L., Bork, P., Bridge, A., Colwell, L., et al. (2023). InterPro in 2022. *Nucleic Acids Res*. 51: D418–D427.

Rahman, K., Coomer, C.A., Majdoul, S., Ding, S.Y., Padilla-Parra, S., and Compton, A.A. (2020). Homology-guided identification of a conserved motif linking the antiviral functions of IFITM3 to its oligomeric state. *eLife* 9: e58537.

Schaffert, L.N. and Carter, W.G. (2020). Do post-translational modifications influence protein aggregation in neurodegenerative diseases: a systematic review. *Brain Sci.* 10: 232.

Smit, J.H., Krishnamurthy, S., Srinivasu, B.Y., Parakra, R., Karamanou, S., and Economou, A. (2021). Probing universal protein dynamics using hydrogen–deuterium exchange mass spectrometry-derived residue-level gibbs free energy. *Anal. Chem*. 93: 12840–12847.

Smith, R.A., Young, J., Weis, J.J., and Weis, J.H. (2006). Expression of the mouse fragilis gene products in immune cells and association with receptor signaling complexes. *Genes Immun.* 7: 113–121.

Smith, S., Weston, S., Kellam, P., and Marsh, M. (2014). IFITM proteins—cellular inhibitors of viral entry. *Curr. Opin. Virol.* 4: 71–77.

Stofella, M., Skinner, S.P., Sobott, F., Houwing-Duistermaat, J., and Paci, E. (2022). High-resolution hydrogen–deuterium protection factors from sparse mass spectrometry data validated by nuclear magnetic resonance measurements. *J. Am. Soc. Mass Spectrom*. 33: 813–822.

Sun, F., Xia, Z., Han, Y., Gao, M., Wang, L., Wu, Y., Sabatier, J.-M., Miao, L., and Cao, Z. (2020). Topology, antiviral functional residues and mechanism of IFITM1. *Viruses* 12: 295.

Tanaka, S.S., Yamaguchi, Y.L., Tsoi, B., Lickert, H., and Tam, P.P.L. (2005). IFITM/mil/Fragilis family proteins IFITM1 and IFITM3 play distinct roles in mouse primordial germ cell homing and repulsion. *Dev. Cell* 9: 745–756.

Weston, S., Czieso, S., White, I.J., Smith, S.E., Kellam, P., and Marsh, M. (2014). A membrane topology model for human interferon inducible transmembrane protein 1. Johannes L, editor. *PLoS ONE* 9: e104341.

Winkler, M., Wrensch, F., Bosch, P., Knoth, M., Schindler, M., Gärtner, S., and Pöhlmann, S. (2019). Analysis of IFITM-IFITM interactions by a flow cytometry-based FRET assay. *IJMS* 20: 3859.

Yánez, D.C., Ross, S., and Crompton, T. (2020). The IFITM protein family in adaptive immunity. *Immunology* 159: 365–372.

Zhao, X., Guo, F., Liu, F., Cuconati, A., Chang, J., Block, T.M., and Guo, J.-T. (2014). Interferon induction of IFITM proteins promotes infection by human coronavirus OC43. *Proc. Natl. Acad. Sci. U.S.A*. 111: 6756–6761.

Zhao, X., Li, J., Winkler, C.A., An, P., and Guo, J.-T. (2019). IFITM genes, variants, and their roles in the control and pathogenesis of viral infections. *Front. Microbiol*. 9: 3228.

Supplementary Material: This article contains supplementary material (https://doi.org/10.1515/hsz-2023-0327).